

pubs.acs.org/JACS Article

Highly Selective Electrochemical Baeyer-Villiger Oxidation through Oxygen Atom Transfer from Water

Yu Mu, Boqiang Chen, Hongna Zhang, Muchun Fei, Tianying Liu, Neal Mehta, David Z. Wang, Alexander J. M. Miller, Paula L. Diaconescu, and Dunwei Wang*



Cite This: https://doi.org/10.1021/jacs.4c02601



ACCESS I

III Metrics & More

Article Recommendations

s Supporting Information

ABSTRACT: The Baeyer–Villiger oxidation of ketones is a crucial oxygen atom transfer (OAT) process used for ester production. Traditionally, Baeyer–Villiger oxidation is accomplished by thermally oxidizing the OAT from stoichiometric peroxides, which are often difficult to handle. Electrochemical methods hold promise for breaking the limitation of using water as the oxygen atom source. Nevertheless, existing demonstrations of electrochemical Baeyer–Villiger oxidation face the challenges of low selectivity. We report in this study a strategy to overcome this challenge. By employing a well-known water oxidation catalyst, Fe₂O₃, we achieved nearly perfect selectivity for the electro-



chemical Baeyer—Villiger oxidation of cyclohexanone. Mechanistic studies suggest that it is essential to produce surface hydroperoxo intermediates (M-OOH, where M represents a metal center) that promote the nucleophilic attack on ketone substrates. By confining the reactions to the catalyst surfaces, competing reactions (e.g., dehydrogenation, carboxylic acid cation rearrangements, and hydroxylation) are greatly limited, thereby offering high selectivity. The surface-initiated nature of the reaction is confirmed by kinetic studies and spectroelectrochemical characterizations. This discovery adds nucleophilic oxidation to the toolbox of electrochemical organic synthesis.

■ INTRODUCTION

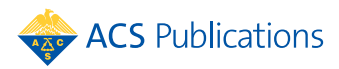
In the pursuit of developing sustainable alternatives for catalysis, 1-6 oxygen atom transfer (OAT) reactions are of great importance for chemical synthesis.⁷ Traditionally, this class of reactions relies on strong oxidants such as peroxyacids, peroxides, or molecular oxygen (O2), which are often difficult to handle.^{8,9} As a result, it presents a challenge for large-scale implementations, such as the preparation of monomers for polymeric materials. Recent advances have inspired researchers to address these challenges by exploiting *in situ* generated oxidants. 12-15 Promising results have been obtained by electrochemically (or photoelectrochemically) oxidizing H₂O to produce intermediates, including oxo species, ^{16,3} peroxo species, 18 hydroperoxo species, 19,20 hydroxyl radicals, 21 and reactive atomic surface oxygen species,²² which can be directly utilized for OAT. For instance, it was recently reported that manganese oxo species generated through an electrochemical approach can efficiently oxidize thioethers to sulfoxides. ¹⁷ Similarly, iron oxo intermediates formed by photoelectrochemical water oxidation were reported to enable OAT reactions through electrophilic attacks. 16

One class of OAT reaction notably missing in these efforts is the Baeyer–Villiger oxidation, an essential process for converting ketones to esters. ^{23–26} A recent attempt to enable this reaction by electrochemistry involved the intermediates of

 ${\rm H_2O_2}$ and resulted in poor selectivity (<50%) and low Faradaic efficiencies (<10%). The key competing factor of this process was understood as the production of hydroxyl radicals ($^{\bullet}$ OH) that would lead to hydroxylation. At the heart of the issue were the relatively poor controls over the oxidation processes, and the overall reaction relied on electrochemically induced chemical reactions away from the surface catalytic site.

We hypothesized that Baeyer–Villiger selectivity could be improved by avoiding high concentrations of reactive oxygen species (ROS) and metastable carboxylic acid cation in solution and instead utilizing the reaction primarily through surface-anchored species. Indeed, surface-adsorbed peroxo ([M $^-$ -OO $^+$]) intermediates generated from water on the PdPtO $_x$ /C catalyst were recently shown to facilitate propylene epoxidation with excellent selectivity. ¹⁸ To achieve Baeyer–Villiger oxidation, we targeted water oxidation catalysts that can produce critical M-OOH intermediates, ^{19,28–30} capable of

Received: February 21, 2024 Revised: April 19, 2024 Accepted: April 22, 2024



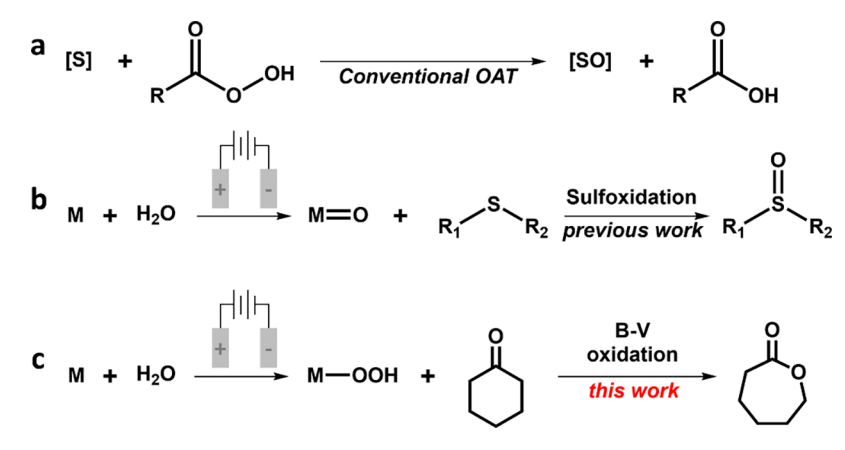


Figure 1. (a) Conventional oxygen-atom-transfer (OAT) reactions. (b) Previous work on electrochemically (or photoelectrochemically) oxidizing H_2O to produce oxidants, e.g., metal oxo (M = O) intermediates, which can be directly utilized for OAT reactions facilitated through electrophilic attacks, e.g., sulfoxidation. (c) Electrochemically catalyzed Baeyer–Villiger oxidation of cyclohexanone through the OAT from water by employing catalysts that can produce M-OOH (this work).

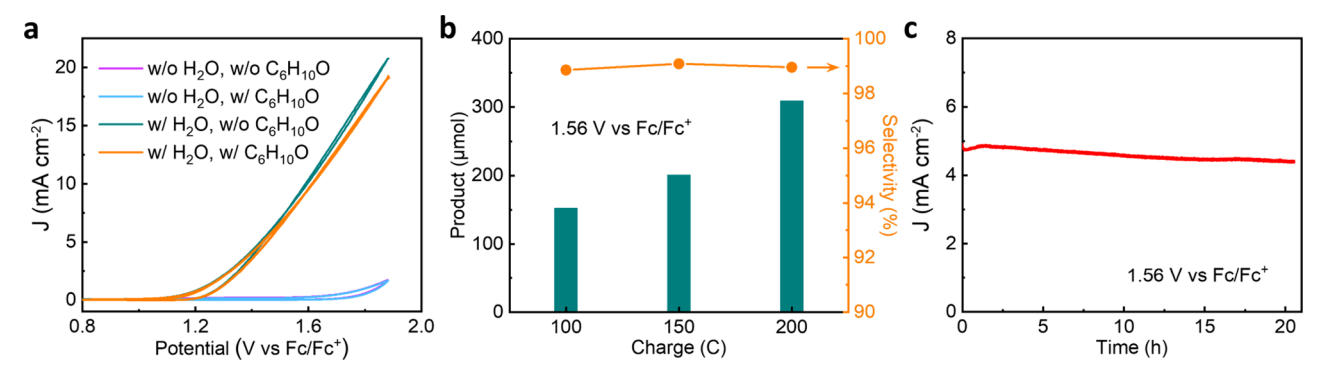


Figure 2. (a) Cyclic voltammogram at a scan rate of 50 mV/s. When present, 60 mM cyclohexanone ($C_6H_{10}O$) and 33.3 vol % water (H_2O) were introduced in acetonitrile (MeCN) containing 0.1 M LiClO₄. (b) Direct electrochemical Baeyer–Villiger oxidation performance and selectivity to ε -caprolactone production by passing different quantities of charges at a constant potential of 1.56 V vs Fc/Fc⁺. (c) Current density collected with potentiostatic electrolysis by passing 200 C charges at 1.56 V vs Fc/Fc⁺, including 60 mM $C_6H_{10}O$, 33.3 vol % H_2O , and 0.1 M LiClO₄ in MeCN.

nucleophilic attacks on the organic ketone substrate, as shown in Figure 1.

We report in this work the application of a known water oxidation catalyst, iron oxide $(Fe_2O_3)^{31-34}$ for the synthesis of ε -caprolactone with ca. 99% selectivity as a benchmark example of Baeyer-Villiger oxidation through electrochemical OAT with H₂O as the oxygen donor. Fe₂O₃ was chosen as a prototypical catalyst to take advantage of its water oxidation activities; other benefits offered by this material include excellent stability, abundance, and low cost. 32,35 For electrode fabrication, a binder-free Fe₂O₃ thin film was deposited onto fluorinated tin oxide (FTO) conductive glass through a solution synthesis method following a previously published procedure (see the Supporting Information, SI, for more details).32 Then, the electrode was used as a working electrode in a one-compartment, three-electrode cell (Figure S2). A typical electrolyte contained acetonitrile (MeCN) as the solvent and 0.1 M lithium perchlorate (LiClO₄) as the support salt, with H₂O (33% by volume) as the oxygen source and cyclohexanone (60 mM) as the substrate. The typical geometric area of the working electrode was ca. 0.6 cm². Carbon paper (ca. 1 cm²) served as the counter electrode. A leakless miniature Ag/AgCl (eDAQ) electrode was used as the reference electrode, calibrated to the ferrocene/ferrocenium (Fc/Fc^{+}) redox potentials (Figure S3).

RESULTS AND DISCUSSION

The first set of experiments carried out was to assess the electrochemical behavior by cyclic voltammetry (CV) without stirring under all combinations of the presence of cyclohexanone and water at a scan rate of 50 mV/s. Strong anodic currents were apparent only in the presence of H₂O, suggesting that H₂O oxidation is preferred under the testing conditions (Figure 2a). The introduction of cyclohexanone marginally reduced the anodic current, presumably by intercepting the water oxidation catalytic cycle through reactions with the Fe-OOH intermediate (vide infra). To characterize the oxidation products, we performed potentiostatic electrolysis at anodic potentials >1.3 V (vs Fc/Fc+; unless noted, all potentials henceforth are relative to this reference). The identity of the products was confirmed by gas chromatography-mass spectrometry (GC-MS, Shimadzu GCMS-QP2010 Ultra) and proton nuclear magnetic resonance (¹H NMR, Varian VNMRS 600) spectroscopy, and the production was quantified by GC-MS. For a typical experiment with 10 C of charge passed (which took ca. 1 h) at 1.56 V, ε -caprolactone was identified as the main product, with few measurable byproducts (e.g., 2-cyclohexen-1-one, 7-oxabicyclo[4.1.0]heptan-2-one, δ -hexanolactone) detected (Figure S4 and Table S1). The byproducts became more detectable after longer reactions (Figure S8 and Table S2), for instance, after ca. 10 h, which corresponded to 100 C of charge passed, they

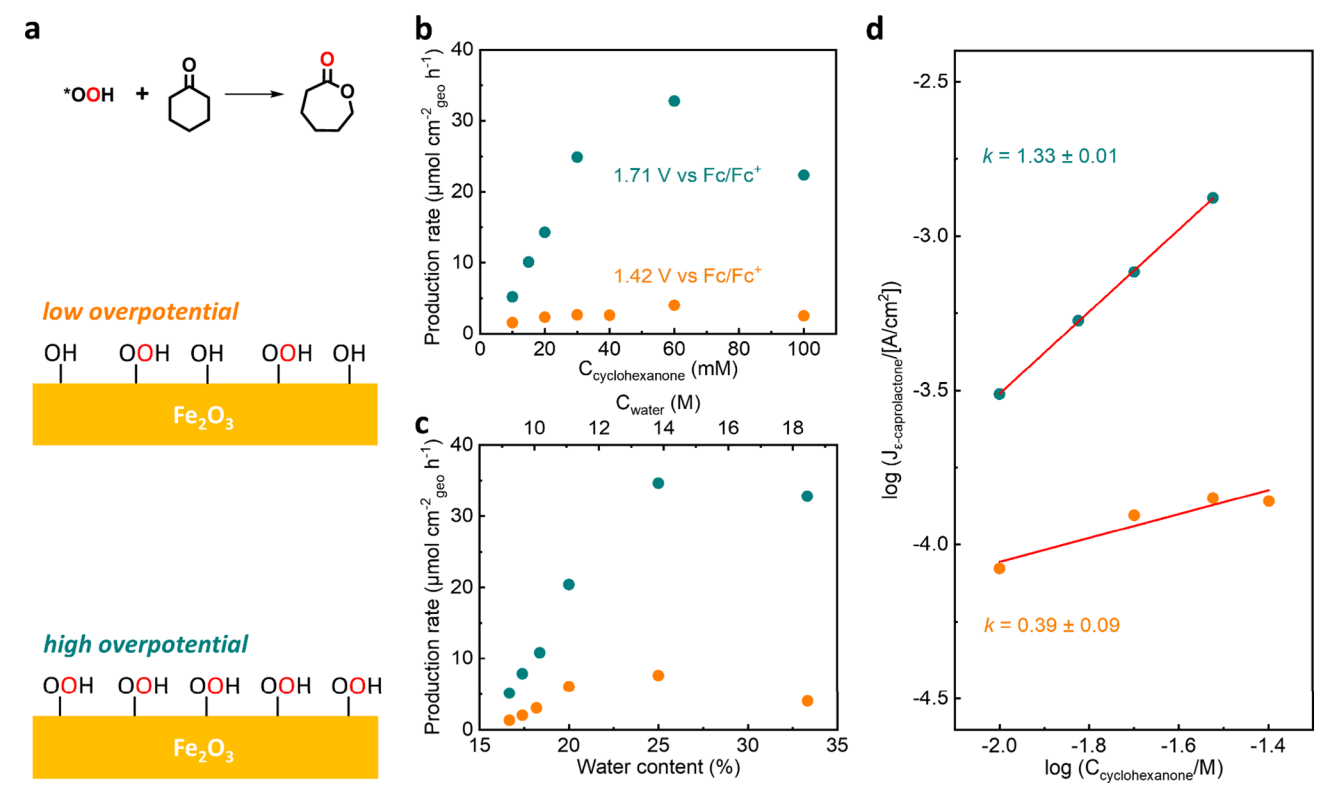


Figure 3. (a) Surface-initiated cyclohexanone oxygenation through *OOH species of which surface-coverage level is varied by applying high (1.71 V vs Fc/Fc⁺, dark cyan) and low (1.42 V vs Fc/Fc⁺, orange) overpotentials. (b) The ε-caprolactone production rate dependence on cyclohexanone concentrations, collected with 33.3 vol % water content. (c) The ε-caprolactone production rate dependence on water concentrations, collected with 60 mM cyclohexanone. (d) Reaction order analysis relative to cyclohexanone concentrations.

amounted to ca. 1% of the total products, with no apparent increase for up to 200 C of charge passed (ca. 20 h) (Figure 2b). Up to ca. 20 h, no obvious changes to the electrode were observed, as confirmed by X-ray measurements (Figure S12). The electrochemical behavior of the electrode also remained stable throughout the reaction with a current density of 4.92 mA/cm² at the beginning, slightly decreasing to 4.40 mA/cm² at the end (Figure 2c). The average current density was 4.60 mA/cm², with ca. 30% Faradaic efficiency in ε -caprolactone production (FE $_{\!\varepsilon\text{-caprolactone}})$ and a normalized production rate of ε -caprolactone of 26 μ mol cm⁻²_{geo} h⁻¹ (where "geo" represents geometric area), and a total conversion of the starting material, cyclohexanone, close to 20% (Figure S13). Furthermore, to test the utility of achieving even greater conversion of the reactant, we fabricated a larger working electrode (ca. 3 cm²) and performed bulk electrolysis for 15 h at 1.56 V. The current passing through the electrolytic cell remained steady at ca. 15 mA throughout the process (Figure S15a). The conversion of cyclohexanone reached ca. 50%, and the yield of ε -caprolactone was determined to be 98.7% (Figure S15b). These results set the stage for future optimizations for even greater conversion.

The high selectivity (close to 99%) for ε -caprolactone is notable and among the best in the literature for electrochemically driven organic synthesis. The result speaks of the exclusivity of substrate activation and its subsequent transformation. In the canonical Baeyer–Villiger oxidation mechanisms, as shown in Figure S16, the substrate is typically activated by the nucleophilic attack of an organic peroxide. The presence of other oxidative species could compete with this mechanism to result in undesired byproducts, as has been

reported in recent Baeyer–Villiger attempts that involved H_2O oxidation.^{27,38} We are therefore inspired to propose that the activation of the ketone substrate takes place exclusively on the surface of the electrode.

To test this hypothesis, the next set of experiments were designed to prove that the reaction is indeed surface initiated. With the premise that *OOH is a key intermediate for the activation of cyclohexanone, we sought to vary its surface coverage and observe how the Baeyer-Villiger oxidation kinetics change (Figure 3a).³⁹ For this purpose, we chose two electrochemical potentials that correspond to different oxidation kinetics: at 1.42 V, the nominal current density as measured in Figure 2a was 4.45 mA/cm², while at 1.71 V, the value was 13.17 mA/cm². At each applied potential, the concentrations of two key reactants, cyclohexanone and H2O, were systematically varied and the rates of Baeyer-Villiger oxidation were observed for the first 10 C of charge passed. The initial increase of the cyclohexanone concentration resulted in a monotonic increase in Baeyer-Villiger oxidation, until the concentration of cyclohexanone reached 60 mM (Figure 3b). Beyond this point, a decrease in Baeyer-Villiger oxidation was apparent and the overall electrochemical current density exhibited a slight decrease with increasing cyclohexanone concentrations (Figure S18a,c). The net result was an increased formation of byproducts (Figure S19). The results are presumably due to an increased competition by direct electrochemical oxidation of cyclohexanone with electrochemically induced chemical oxidation, which in turn was caused by the increased availability of cyclohexanone. Importantly, the rate of Baeyer-Villiger oxidation was consistently higher at 1.71 V than at 1.42 V for all cyclohexanone concentrations.

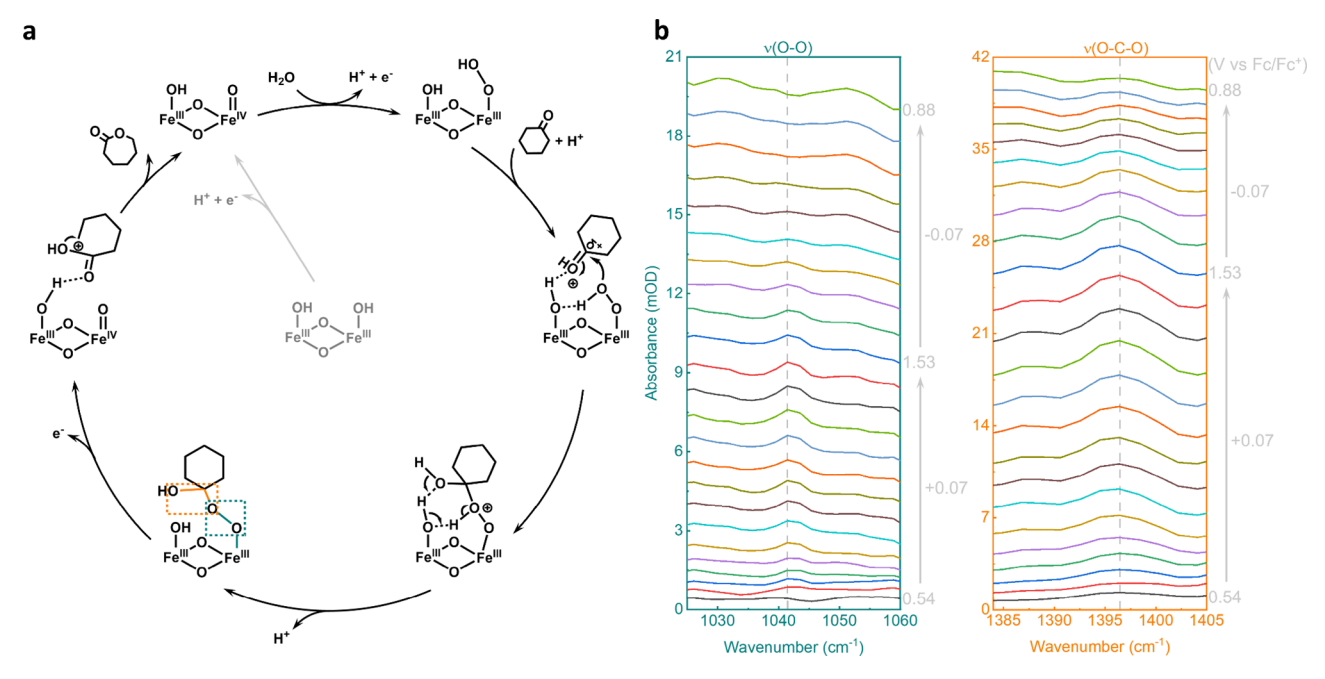


Figure 4. (a) Proposed catalytic cycle for the electrochemical Baeyer–Villiger oxidation of cyclohexanone. The Criegee adduct ([Fe–O–O-R]) intermediate displays two representative stretching modes from O–O and O–C–O, respectively. *Operando* ATR-SEIRAS measurements of the detections of (b) O–O and (c) O–C–O stretching modes within [Fe–O–O-R]. They are ascribed to two potential-dependent vibrational bands centered at 1042 and 1396 cm⁻¹.

Similarly, a monotonic increase of the Baeyer–Villiger oxidation rate with increasing $\rm H_2O$ concentration was observed up to ca. 25%, beyond which a decrease was apparent (Figure 3c). The results may be attributed to increased $\rm O_2$ evolution at higher $\rm H_2O$ concentrations, which competes with Baeyer–Villiger oxidation.

This set of data allowed us to extract the apparent reaction orders as a function of the cyclohexanone concentrations. As shown in Figure 3d, two different behaviors were observed. At 1.71 V, an apparent reaction order of 1.33 was determined, whereas at 1.42 V, it substantially decreased to <1. These results provided additional support for the surface-initiated reaction mechanism.¹⁸ At high applied potentials, the water oxidation kinetics is fast and the surface is expected to be saturated with *OOH species. Consequently, the overall Baeyer-Villiger oxidation rate is limited by the availability of cyclohexanone molecules. A pseudo-first-order characteristic was thus observed relative to the cyclohexanone concentration. By comparison, at low applied potentials, a relatively slow H₂O oxidation is expected, implying a relatively low coverage of surface *OOH species.³⁹ In this case, the overall reaction rate would be largely determined by the availability of surface *>OOH species (Figure 3c). 18 As such, the availability of cyclohexanone molecules is not the only limiting factor to the overall reaction rates. Under the likely assumption that the steady-state concentration of surface *OOH species might be influenced by the presence of cyclohexanone, the apparent reaction order would be less than one relative to cyclohexanone, which is consistent with our observation. Taken together, these data provide evidence to support that the Baeyer-Villiger oxidation is surface initiated.

Next, we performed H₂¹⁸O labeling experiments to show that the O in the Baeyer–Villiger oxidation products is indeed transferred from H₂O.¹⁶ For this purpose, H₂¹⁸O (97%, Medical Isotopes) was used and potentiostatic electrolysis was performed under electrochemical conditions identical to those

described above. We found that the prominent molecular ion peak of ε -caprolactone featured a mass-to-charge ratio (m/z)of 116 when H₂¹⁸O was used, compared to 114 when H₂¹⁶O was employed (Figure S21), providing direct evidence that the Baeyer-Villiger oxidation was enabled by H₂O oxidation. Moreover, the dominant ion peaks of the C5H8O fragment (m/z = 84) and C₃H₃O fragment (m/z = 55) were also shifted by 2 m/z units, clearly supporting the substitution of 16 O with ¹⁸O in these fragments. Considering that C₅H₈O and C₃H₃O fragments report on the oxygen from the carbonyl group in ε caprolactone, 40 we understand the Baeyer-Villiger oxidation to proceed through an electron-transfer-based O-O bond dissociation mechanism (Figure 4a and Figure S28c). A competing possibility is that the surface-anchored intermediate can go through proton migration to produce ε -caprolactone that would lead to the OAT to the second oxygen atom rather than the oxygen atom within the carbonyl group (Figure S22). Such a possibility is contradictory to the MS observations and is therefore unlikely.

With all of the information available so far, we propose the overall catalytic cycle for the electrochemical Baeyer-Villiger oxidation as follows. The reaction initiates with the formation of metal oxo (M=O) species on the surface of the electrode, which can be readily transformed to hydroperoxo (M-OOH) through oxidation in the presence of H_2O . All 41,42 Similar to how peroxyacids activate ketones in canonical Baeyer-Villiger oxidation, M-OOH engages with the ketone substrate via nucleophilic attack. Subsequently, a hydrogen-bonding rearrangement takes place. 43 After deprotonation, the surfaceanchored intermediate known as the Criegee adduct ([Fe-O-O-R], where R represents the organic functional group) is formed. In the final oxidation step, the O-O bond dissociation occurs, resulting in a transformation into a surface-adsorbed carboxylic acid cation. A subsequent rearrangement promptly releases the product and recovers M=O for the next catalytic

cycle. To further support the proposed catalytic cycle, we next performed attenuated total reflectance surface-enhanced infrared absorption spectroscopy (ATR-SEIRAS, see the SI for experimental details) in operando. 39,44,45 The IR spectra in Figure 4b clearly show two vibrational bands centered at around 1042 and 1396 cm⁻¹ (see Figure S26 for the full spectra). They are ascribed to the O-O and O-C-O stretching modes within [Fe-O-O-R], respectively (see the SI for detailed discussions). 29,44,46,47 The reversibility of these signals with changing potentials was further confirmed by filtering out static background absorbance with phase sensitive detection (Figure S27).³⁹ The successful detection of the [Fe-O-O-R] intermediate lends additional strong support to the proposed mechanisms. It is important to note that the nucleophilic attack by the M-OOH species on the substrate is the key enabling factor for the Baeyer-Villiger oxidation. While electrophilic M=O species could also active organic substrates and enable OAT, as has been reported recently by several groups, 16,17,48,49 these mechanisms would not enable the Baeyer-Villiger transformation. As such, our results represent an important advancement in electrochemically based chemical synthesis. It is last noted that the Baeyer-Villiger oxidation could, in principle, be enabled by M-OO* (superoxo radicals), as well. If so, it would imply that the OAT takes place at a later stage of the H2O oxidation reactions. The difference notwithstanding, all discussions presented here would still be valid should this mechanism be the preferred one. However, we consider such a mechanism less likely for Fe₂O₃-based catalysts. This is because H₂O oxidation by Fe₂O₃ is known to be kinetically limited by early steps. 50 To fully resolve the potential differences, additional research will likely be needed, which is beyond the scope of this work.

We also note that the mechanisms proposed here are expected to be applicable to other substrates, as demonstrated by the highly selective production observed through the Baeyer–Villiger oxidation of cyclopentanone and 2-methyl-cyclohexanone in our preliminary trials (Figure S29). Moreover, this mechanism may be extended to other H_2O oxidation catalysts, such as iridium oxide (IrO_x) and cobalt oxyhydroxide $(CoO_x(OH)_y)$, 30,39 which feature the generation of M-OOH intermediates, which have shown ca. 90% selectivity in Baeyer–Villiger oxidation under the conditions optimized for Fe_2O_3 (Figure S30 and Table S2; see the SI for detailed discussions). Together, they speak to the general applicability of the reported strategy in enabling the use of OAT by electrochemical water oxidation.

CONCLUSIONS

In summary, we achieved highly selective electrochemical Baeyer–Villiger oxidation through OAT from water. It was hypothesized that M-OOH serves as a crucial intermediate, which facilitates a surface-initiated catalytic pathway through nucleophilic attack to activate the ketone substrates. With cyclohexanone as a prototypical substrate, and Fe₂O₃ as an OAT catalyst, we obtained ca. 99% selectivity for ε -caprolactone production. The overall Faradaic efficiency was ca. 30%, with O₂ evolution as the main competing reaction, and no other significant organic byproducts were detected. Our preliminary results showed that the proposed mechanisms are broadly applicable to the Baeyer–Villiger oxidation of other cyclic ketones (e.g., cyclopentanone and 2-methylcyclohexanone). The mechanism is also extendable to other H₂O

oxidation catalysts, such as iridium oxide (IrO_x) and cobalt oxyhydroxide ($CoO_x(OH)_y$), which feature effective generation of M-OOH intermediates. The results reported here are expected to contribute to the efforts for electrochemical OAT and/or other types of oxidation reactions. Future research should be directed toward understanding how to further minimize O_2 evolution so as to improve the efficiency of charge utilizations.

ASSOCIATED CONTENT

Supporting Information

The Supporting Information is available free of charge at https://pubs.acs.org/doi/10.1021/jacs.4c02601.

Detailed experimental procedures, additional results and discussions, including characterizations, mechanistic details, and electrochemical studies (PDF)

AUTHOR INFORMATION

Corresponding Author

Dunwei Wang — Department of Chemistry, Merkert Chemistry Center, Boston College, Chestnut Hill, Massachusetts 02467, United States; orcid.org/0000-0001-5581-8799; Email: dunwei.wang@bc.edu

Authors

Yu Mu — Department of Chemistry, Merkert Chemistry Center, Boston College, Chestnut Hill, Massachusetts 02467, United States; orcid.org/0009-0007-6277-7201

Boqiang Chen – Department of Chemistry, Merkert Chemistry Center, Boston College, Chestnut Hill, Massachusetts 02467, United States; orcid.org/0000-0002-1754-2055

Hongna Zhang — Department of Chemistry, Merkert Chemistry Center, Boston College, Chestnut Hill, Massachusetts 02467, United States

Muchun Fei – Department of Chemistry, Merkert Chemistry Center, Boston College, Chestnut Hill, Massachusetts 02467, United States

Tianying Liu — Department of Chemistry, Merkert Chemistry Center, Boston College, Chestnut Hill, Massachusetts 02467, United States; orcid.org/0000-0001-9165-308X

Neal Mehta – Department of Chemistry, Merkert Chemistry Center, Boston College, Chestnut Hill, Massachusetts 02467, United States

David Z. Wang — Department of Chemistry, Merkert Chemistry Center, Boston College, Chestnut Hill, Massachusetts 02467, United States

Alexander J. M. Miller — Department of Chemistry, University of North Carolina at Chapel Hill, Chapel Hill, North Carolina 27599, United States; orcid.org/0000-0001-9390-3951

Paula L. Diaconescu — Department of Chemistry and Biochemistry, University of California, Los Angeles, Los Angeles, California 90095, United States; orcid.org/0000-0003-2732-4155

Complete contact information is available at: https://pubs.acs.org/10.1021/jacs.4c02601

Notes

The authors declare no competing financial interest.

ACKNOWLEDGMENTS

This material is based on work supported by the National Science Foundation as part of the Center for Integrated Catalysis (CHE-2023955). NMR spectroscopy at BC was carried out in Merkert Chemistry Center NMR Core Laboratory and supported by the NSF MRI award CHE2117246 and the NIH HEI-S10 award 1S10OD026910-01A1. SEM measurements were carried out in a BC clean room. X-ray measurements were conducted in Materials Characterization Core (MCC) at BC. We thank Dr. Yucheng Yuan for her help with ATR-FTIR measurements in MCC at BC. We thank Prof. Dr. Matthias M. Waegele for his help with the spectroelectrochemical measurements. We thank Dr. Wei Li for her help with reviewing the feasibility of Fe₂O₃ and the manuscript.

REFERENCES

- (1) Deng, S.; Jolly, B. J.; Wilkes, J. R.; Mu, Y.; Byers, J. A.; Do, L. H.; Miller, A. J. M.; Wang, D.; Liu, C.; Diaconescu, P. L. Spatiotemporal Control for Integrated Catalysis. *Nat. Rev. Methods Primers* **2023**, 3 (1), 28.
- (2) Dodge, H. M.; Natinsky, B. S.; Jolly, B. J.; Zhang, H.; Mu, Y.; Chapp, S. M.; Tran, T. V.; Diaconescu, P. L.; Do, L. H.; Wang, D.; Liu, C.; Miller, A. J. M. Polyketones from Carbon Dioxide and Ethylene by Integrating Electrochemical and Organometallic Catalysis. ACS Catal. 2023, 13 (7), 4053–4059.
- (3) Tran, T. V.; Shen, Y.; Nguyen, H. D.; Deng, S.; Roshandel, H.; Cooper, M. M.; Watson, J. R.; Byers, J. A.; Diaconescu, P. L.; Do, L. H. N-Carboxyanhydrides Directly from Amino Acids and Carbon Dioxide and Their Tandem Reactions to Therapeutic Alkaloids. *Green Chem.* 2022, 24 (23), 9245–9252.
- (4) Nguyen, H. D.; Tran, T. V.; Taylor, C. R.; Campbell, D. T.; Harkins, D. I.; Do, L. H. 2-Azaaryl-1-methylpyridinium Halides: Aqueous-Soluble Activating Reagents for Efficient Amide Coupling in Water. ACS Sustainable Chem. Eng. 2022, 10 (39), 12968–12974.
- (5) Qi, M.; Zhang, H.; Dong, Q.; Li, J.; Musgrave, R. A.; Zhao, Y.; Dulock, N.; Wang, D.; Byers, J. A. Electrochemically Switchable Polymerization from Surface-anchored Molecular Catalysts. *Chem. Sci.* **2021**, *12* (26), 9042–9052.
- (6) Shen, Y.; Mu, Y.; Wang, D.; Liu, C.; Diaconescu, P. L. Tuning Electrode Reactivity through Organometallic Complexes. *ACS Appl. Mater. Interfaces* **2023**, *15* (24), 28851–28878.
- (7) Holm, R. H. Metal-Centered Oxygen Atom Transfer Reactions. Chem. Rev. 1987, 87 (6), 1401–1449.
- (8) Renz, M.; Meunier, B. 100 Years of Baeyer-Villiger Oxidations. *Eur. J. Org. Chem.* **1999**, 1999 (4), 737-750.
- (9) Stamoulis, A. G.; Bruns, D. L.; Stahl, S. S. Optimizing the Synthetic Potential of O₂: Implications of Overpotential in Homogeneous Aerobic Oxidation Catalysis. *J. Am. Chem. Soc.* **2023**, 145 (32), 17515–17526.
- (10) Ren, J. M.; McKenzie, T. G.; Fu, Q.; Wong, E. H.; Xu, J.; An, Z.; Shanmugam, S.; Davis, T. P.; Boyer, C.; Qiao, G. G. Star Polymers. *Chem. Rev.* **2016**, *116* (12), 6743–836.
- (11) Zhang, X.; Fevre, M.; Jones, G. O.; Waymouth, R. M. Catalysis as an Enabling Science for Sustainable Polymers. *Chem. Rev.* **2018**, 118 (2), 839–885.
- (12) Sheng, H.; Janes, A. N.; Ross, R. D.; Hofstetter, H.; Lee, K.; Schmidt, J. R.; Jin, S. Linear Paired Electrochemical Valorization of Glycerol Enabled by the Electro-Fenton Process Using a Stable NiSe₂ Cathode. *Nat. Catal.* **2022**, *5* (8), 716–725.
- (13) Lewis, R. J.; Ueura, K.; Liu, X.; Fukuta, Y.; Davies, T. E.; Morgan, D. J.; Chen, L.; Qi, J.; Singleton, J.; Edwards, J. K.; Freakley, S. J.; Kiely, C. J.; Yamamoto, Y.; Hutchings, G. J. Highly Efficient Catalytic Production of Oximes from Ketones Using in situ-Generated H₂O₂. Science **2022**, 376 (6593), 615–620.
- (14) Jin, Z.; Wang, L.; Zuidema, E.; Mondal, K.; Zhang, M.; Zhang, J.; Wang, C.; Meng, X.; Yang, H.; Mesters, C.; Xiao, F. S.

- Hydrophobic Zeolite Modification for in situ Peroxide Formation in Methane Oxidation to Methanol. *Science* **2020**, *367* (6474), 193–197.
- (15) Fei, M.; Williams, B.; Wang, L.; Li, H.; Yuan, Y.; Wilkes, J. R.; Liu, T.; Mu, Y.; Huang, J.; Nyakuchena, J.; Huang, J.; Li, W.; Wang, D. Highly Selective Photocatalytic Methane Coupling by Au-Modified Bi₂WO₆. ACS Catal. **2024**, *14* (3), 1855–1861.
- (16) Zhao, Y.; Deng, C.; Tang, D.; Ding, L.; Zhang, Y.; Sheng, H.; Ji, H.; Song, W.; Ma, W.; Chen, C.; Zhao, J. α -Fe₂O₃ as a Versatile and Efficient Oxygen Atom Transfer Catalyst in Combination with H₂O as the Oxygen Source. *Nat. Catal.* **2021**, *4* (8), 684–691.
- (17) Hoque, M. A.; Gerken, J. B.; Stahl, S. S. Synthetic Dioxygenase Reactivity by Pairing Electrochemical Oxygen Reduction and Water Oxidation. *Science* **2024**, 383 (6679), 173–178.
- (18) Chung, M.; Maalouf, J. H.; Adams, J. S.; Jiang, C.; Roman-Leshkov, Y.; Manthiram, K. Direct Propylene epoxidation via Water Activation over Pd-Pt Electrocatalysts. *Science* **2024**, 383 (6678), 49–55
- (19) Tang, H.; Zhou, H.; Pan, Y.; Zhang, J.; Cui, F.; Li, W.; Wang, D. Single-Atom Manganese-Catalyzed Oxygen Evolution Drives the Electrochemical Oxidation of Silane to Silanol. *Angew. Chem., Int. Ed.* **2024**, *63* (3), No. e202315032.
- (20) Sun, Y.; Li, X.; Yang, M.; Xu, W.; Xie, J.; Ding, M. Highly Selective Electrocatalytic Oxidation of Benzyl C–H Using Water as Safe and Sustainable Oxygen Source. *Green Chem.* **2020**, 22 (21), 7543–7551.
- (21) Kang, Y.; Gu, Z.; Ma, B.; Zhang, W.; Sun, J.; Huang, X.; Hu, C.; Choi, W.; Qu, J. Unveiling the Spatially Confined Oxidation Processes in Reactive Electrochemical Membranes. *Nat. Commun.* **2023**, *14* (1), 6590.
- (22) Zhang, H.; Li, C.; Lu, Q.; Cheng, M. J.; Goddard, W. A., III Selective Activation of Propane Using Intermediates Generated during Water Oxidation. *J. Am. Chem. Soc.* **2021**, *143* (10), 3967–3974.
- (23) Uyanik, M.; Ishihara, K. Baeyer–Villiger Oxidation Using Hydrogen Peroxide. *ACS Catal.* **2013**, 3 (4), 513–520.
- (24) Strukul, G. Transition Metal Catalysis in the Baeyer-Villiger Oxidation of Ketones. *Angew. Chem., Int. Ed.* **1998**, 37 (9), 1198–1209.
- (25) ten Brink, G. J.; Arends, I. W.; Sheldon, R. A. The Baeyer-Villiger Reaction: New Developments toward Greener Procedures. *Chem. Rev.* **2004**, *104* (9), 4105–24.
- (26) Michelin, R. A.; Sgarbossa, P.; Scarso, A.; Strukul, G. The Baeyer–Villiger Oxidation of Ketones: A Paradigm for the Role of Soft Lewis Acidity in Homogeneous Catalysis. *Coord. Chem. Rev.* **2010**, 254 (5–6), 646–660.
- (27) Herman, A.; Mathias, J.-L.; Neumann, R. Electrochemical Formation and Activation of Hydrogen Peroxide from Water on Fluorinated Tin Oxide for Baeyer–Villiger Oxidation Reactions. *ACS Catal.* **2022**, *12* (7), 4149–4155.
- (28) Nakamura, R.; Nakato, Y. Primary Intermediates of Oxygen Photoevolution Reaction on TiO₂ (Rutile) Particles, Revealed by in situ FTIR Absorption and Photoluminescence Measurements. *J. Am. Chem. Soc.* **2004**, *126* (4), *1290*–8.
- (29) Zhang, M.; de Respinis, M.; Frei, H. Time-Resolved Observations of Water Oxidation Intermediates on a Cobalt Oxide Nanoparticle Catalyst. *Nat. Chem.* **2014**, *6* (4), 362–7.
- (30) Lang, C.; Li, J.; Yang, K. R.; Wang, Y.; He, D.; Thorne, J. E.; Croslow, S.; Dong, Q.; Zhao, Y.; Prostko, G.; Brudvig, G. W.; Batista, V. S.; Waegele, M. M.; Wang, D. Observation of a Potential-Dependent Switch of Water-Oxidation Mechanism on Co-Oxide-Based Catalysts. *Chem.* **2021**, *7* (8), 2101–2117.
- (31) Mesa, C. A.; Francas, L.; Yang, K. R.; Garrido-Barros, P.; Pastor, E.; Ma, Y.; Kafizas, A.; Rosser, T. E.; Mayer, M. T.; Reisner, E.; Gratzel, M.; Batista, V. S.; Durrant, J. R. Multihole Water Oxidation Catalysis on Haematite Photoanodes Revealed by Operando Spectroelectrochemistry and DFT. *Nat. Chem.* **2020**, *12* (1), 82–89.
- (32) Jang, J. W.; Du, C.; Ye, Y.; Lin, Y.; Yao, X.; Thorne, J.; Liu, E.; McMahon, G.; Zhu, J.; Javey, A.; Guo, J.; Wang, D. Enabling

- Unassisted Solar Water Splitting by Iron Oxide and Silicon. *Nat. Commun.* **2015**, *6*, 7447.
- (33) Liu, T.; Li, W.; Wang, D. Z.; Luo, T.; Fei, M.; Shin, D.; Waegele, M. M.; Wang, D. Low Catalyst Loading Enhances Charge Accumulation for Photoelectrochemical Water Splitting. *Angew. Chem., Int. Ed.* **2023**, 62 (34), No. e202307909.
- (34) Li, W.; Yang, K. R.; Yao, X.; He, Y.; Dong, Q.; Brudvig, G. W.; Batista, V. S.; Wang, D. Facet-Dependent Kinetics and Energetics of Hematite for Solar Water Oxidation Reactions. *ACS Appl. Mater. Interfaces* **2019**, *11* (6), 5616–5622.
- (35) Klahr, B.; Gimenez, S.; Fabregat-Santiago, F.; Bisquert, J.; Hamann, T. W. Electrochemical and Photoelectrochemical Investigation of Water Oxidation with Hematite Electrodes. *Energy Environ. Sci.* **2012**, *5* (6), 7626–1861.
- (36) Sun, Y.; Shin, H.; Wang, F.; Tian, B.; Chiang, C. W.; Liu, S.; Li, X.; Wang, Y.; Tang, L.; Goddard, W. A., III; Ding, M. Highly Selective Electrocatalytic Oxidation of Amines to Nitriles Assisted by Water Oxidation on Metal-Doped α -Ni(OH)₂. *J. Am. Chem. Soc.* **2022**, 144 (33), 15185–15192.
- (37) Frontana-Uribe, B. A.; Little, R. D.; Ibanez, J. G.; Palma, A.; Vasquez-Medrano, R. Organic Electrosynthesis: A Promising Green Methodology in Organic Chemistry. *Green Chem.* **2010**, *12* (12), 2099.
- (38) Maalouf, J. H.; Jin, K.; Yang, D.; Limaye, A. M.; Manthiram, K. Kinetic Analysis of Electrochemical Lactonization of Ketones Using Water as the Oxygen Atom Source. *ACS Catal.* **2020**, *10* (10), 5750–5756.
- (39) Zhang, H.; Chen, B.; Liu, T.; Brudvig, G. W.; Wang, D.; Waegele, M. M. Infrared Spectroscopic Observation of Oxo- and Superoxo-Intermediates in the Water Oxidation Cycle of a Molecular Ir Catalyst. J. Am. Chem. Soc. 2024, 146 (1), 878–883.
- (40) Tabet, J. C.; Doan, D.; Longeray, R.; Fraisse, D.; Suon, K. Molecular Isomerization and Fragmentation of Caprolactone upon Electron Impact. *Int. J. Mass Spectrom. Ion Phys.* **1983**, 47, 407–410.
- (41) Shaffer, D. W.; Xie, Y.; Concepcion, J. J. O-O Bond Formation in Ruthenium-Catalyzed Water Oxidation: Single-Site Nucleophilic Attack vs. O-O Radical Coupling. *Chem. Soc. Rev.* **2017**, 46 (20), 6170–6193.
- (42) Tian, B.; Shin, H.; Liu, S.; Fei, M.; Mu, Z.; Liu, C.; Pan, Y.; Sun, Y.; Goddard, W. A., III; Ding, M. Double-Exchange-Induced in situ Conductivity in Nickel-Based Oxyhydroxides: An Effective Descriptor for Electrocatalytic Oxygen Evolution. *Angew. Chem., Int. Ed.* **2021**, *60* (30), 16448–16456.
- (43) Westendorff, K. S.; Hulsey, M. J.; Wesley, T. S.; Roman-Leshkov, Y.; Surendranath, Y. Electrically Driven Proton Transfer Promotes Bronsted Acid Catalysis by Orders of Magnitude. *Science* **2024**, 383 (6684), 757–763.
- (44) Zandi, O.; Hamann, T. W. Determination of Photoelectrochemical Water Oxidation Intermediates on Haematite Electrode Surfaces Using Operando Infrared Spectroscopy. *Nat. Chem.* **2016**, *8* (8), 778–83.
- (45) Rao, R. R.; Kolb, M. J.; Giordano, L.; Pedersen, A. F.; Katayama, Y.; Hwang, J.; Mehta, A.; You, H.; Lunger, J. R.; Zhou, H.; Halck, N. B.; Vegge, T.; Chorkendorff, I.; Stephens, I. E. L.; Shao-Horn, Y. Operando Identification of Site-Dependent Water Oxidation Activity on Ruthenium Dioxide Single-Crystal Surfaces. *Nat. Catal.* **2020**, *3* (6), 516–525.
- (46) Gao, X.; Metge, D. W.; Ray, C.; Harvey, R. W.; Chorover, J. Surface Complexation of Carboxylate Adheres Cryptosporidium Parvum Oocysts to the Hematite-Water Interface. *Environ. Sci. Technol.* **2009**, 43 (19), 7423–9.
- (47) Zhang, Y.; Zhang, H.; Liu, A.; Chen, C.; Song, W.; Zhao, J. Rate-Limiting O-O Bond Formation Pathways for Water Oxidation on Hematite Photoanode. *J. Am. Chem. Soc.* **2018**, *140* (9), 3264–3269.
- (48) Chung, M.; Jin, K.; Zeng, J. S.; Ton, T. N.; Manthiram, K. Tuning Single-Atom Dopants on Manganese Oxide for Selective Electrocatalytic Cyclooctene epoxidation. *J. Am. Chem. Soc.* **2022**, *144* (38), 17416–17422.

- (49) Das, A.; Nutting, J. E.; Stahl, S. S. Electrochemical C-H Oxygenation and Alcohol Dehydrogenation involving Fe-Oxo Species Using Water as the Oxygen Source. *Chem. Sci.* **2019**, *10* (32), 7542–7548.
- (50) Corby, S.; Rao, R. R.; Steier, L.; Durrant, J. R. The Kinetics of Metal Oxide Photoanodes from Charge Generation to Catalysis. *Nat. Rev. Mater.* **2021**, *6* (12), 1136–1155.